



Supplement of

Applying dynamical systems techniques to real ocean drifters

Irina I. Rypina et al.

Correspondence to: Irina I. Rypina (irypina@whoi.edu)

The copyright of individual parts of the supplement might differ from the article licence.

Supplementary material

Navy Coastal Ocean Model (NCOM) – based results

The high-resolution operational forecasting model NCOM (Navy Coastal Ocean Model, Martin, 2000) has been widely used for the studies of the Gulf of Mexico (Poje et al., 2014; Jacobs et al., 2014; Beron-Vera et al., 2016; Ozgokmen et al., 2021). The model fields are available every 3 hours for the entire Gulf of Mexico with a horizontal resolution of 1 km. NCOM includes tides and river run off, which are two of the dominant forcing mechanisms in the northeastern GOM (the site of the SPLASH experiment), and has been shown to realistically reproduce the typical ocean circulation features in the region, such as the transient, rapidly-varying submesoscale eddies of both cyclonic and anticyclonic rotation and the strong and rapidly evolving density fronts formed by the confluence of the freshwater run-off from the coast with the saltier waters from the Gulf of Mexico (Jacobs et al., 2014; Ozgokmen et al., 2021). Importantly, the model captured both the anticyclonic circulation and the two density fronts that were present in the area at the time of the SPLASH drifter experiment and that influenced the behavior of the drifters.

Because CARTE drifters used during the SPLASH deployment were shallow and sampled approximately the top 60 cm of the water column, we used the surface model fields to advect the simulated drifters. In order to simulate the motions of simulated drifters in the NCOM model, we used the standard variable-step 4th order Runge-Kutta integration method (MATLAB's built-in function "ode45") with a bi-linear velocity interpolation in time and space between the model grid points (the same integration and interpolation schemes were used in Rypina et al. (2021)).

Density variations, topography, and wind forcing are generally all important factors in setting the circulation and transport in this geographical region of the Gulf of Mexico. Inspection of the model density fields (Fig. S1) suggested that 2 density features had a particularly strong influence on the movement of SPLASH drifters: the dense water filament (red) that affected the northern group of drifters during the splitting event around days 0.9-1.25, and the light water coastal plume (blue) that affected the southern group of drifters from day 1.25 and onward. Specifically, the distribution of drifters on days 1.25 through day 2 after deployment was roughly aligned with the density fronts associated with the warm and cold filaments, which formed around day 1 when the drifters were approaching the coast and which influenced the off-shore motion of the drifters during days 1.25-2. However, as is typical for numerical models, the exact location and timing of both of these features differed slightly from the real ocean circulation, as is evident from the slight misalignment between the SPLASH drifters and the model fronts. (Such slight mismatch between the modeled and observed flow features is common for even the highest-resolution state-of-the-art data-assimilative oceanographic models, which tend to qualitatively reproduce the observed features but miss the small-scale details (see Rypina et al. (2021) for an example of such behavior in the Western Mediterranean Sea)). Because of these slight differences, simulated drifters released at the exact times and locations of the real drifters experienced a more northward advection during the first day after deployment and, as a result, missed the formation of the density fronts (Fig. S2a) and experienced less spreading and a weaker off-shore advection. This mismatch can be mitigated by shifting the release locations of simulated drifters about 6 km to the southeast, which allowed the simulated drifters to remain within the

anticyclonic circulation during the first day and to arrive at the coast when the density fronts were still present (Fig. S2b). The simulated drifters then aligned themselves with the fronts and moved off-shore to the southwest, in a qualitative agreement with the real drifters. Because the behavior of the simulated drifters released at the shifted location was in a better qualitative agreement with real drifters, we have proceeded with this shifted drifter release in our subsequent analysis. Just like the real drifters, the simulated drifters from the shifted release initially started moving anticyclonically around the recirculation feature towards the coast. The drifters then split into a smaller northern and larger southern group, the northern group aligned along the coast, and then the entire drifter ensemble proceeded offshore, all in qualitative agreement with real drifters. However, simulated drifters moved slower than real drifters during the initial and intermediate stages, i.e., it took them longer to approach the coast and form the along-shore filament. By day 1.5, simulated drifters started approaching the coast but they didn't fully form the characteristic filament until day 2. After that, their off-shore movement was comparable to that for real drifters. Thus, we chose 2 days for simulated drifters (instead of 1 day for real drifters) as the representative time for the intermediate stage, and then allowed them the same amount of time (i.e., 2 days since formation of filament) to progress offshore as we did for real drifters, thus yielding 4 days as the analysis time for the third stage. In Figs. S3-S10, we show FTLEs, L , CD , V_{en} , $LAVD$, D , and spectral clusters computed using segments of simulated trajectories from $t_{start} = 0$ days to $t_{end} = 0.5, 2,$ and 4 days, respectively. These are the simulated-drifter-based counterparts of Figs. 3-9. Then we re-computed the same quantities using dense regularly-spaced orthogonal grids of simulated drifters in order to investigate possible biases arising due to the limited

number of SPLASH drifters and the non-regularity and non-orthogonality of the SPLASH release grid. In the remainder of the Supplement we will refer to the model fields computed using simulated SPLASH-like drifters as the ‘‘SPLASH-like’’ simulations, and to the model fields computed using the dense regular orthogonal grids as the ‘‘dense-grid’’ model fields.

FTLEs (Fig. S3). At the initial stage of motion ($t_{end} = 0.5$ days), the SPLASH-like FTLEs showed a zonal swath of larger values (where the drifters diverged more strongly) extending from the western corner of the release domain, with smaller FTLEs to the north and south of it. There was also a small region of negative FTLEs in the north, where drifters converged closer together, instead of separating from each other. The distribution of drifters at 0.5 days in the top middle panel of Fig. S3 bears some resemblance to that in Fig. 3, specifically, the separations between dots in the middle of the domain were larger than in the east and west. However, FTLEs were much smoother in the model and almost exclusively positive, compared to noisier mixed-sign FTLEs in observations. Comparison with the dense-grid model FTLEs (second row) showed excellent agreement, as both the zonal swath of the large FTLEs extending from the west and the negative-FTLE region in the north were clearly present, and the magnitudes of FTLEs were also comparable between the two cases.

At the intermediate stage of motion ($t_{end} = 2$ days), when the simulated drifters approached the coast, split to the north and south and formed an elongated along-shore filament, the SPLASH-like FTLEs looked more complex than at the initial stage, but several features could still be easily teased out. In the western half of the release domain, a zonal filament of larger FTLEs values (similar to the one at 0.5 days) extending from the western corner was still visible, with smaller values to the north

and south from it. In the eastern half of the domain, the FTLEs structures were less clear, with intermingled small clusters of high and low FTLEs located next to each other. Dense-grid model FTLEs revealed the presence of several maximizing ridges within the domain – the elongated filament extending from the west at about 29.025°N (that was also present at 0.5 days), the S-shaped ridge entering the domain from the east at about 29.07°N , and a strong ridge in the south extending across the entire domain (plus some other shorter and weaker ridges in other parts of the domain). Because the distances between these individual ridges were in some cases comparable to the spacing between SPLASH drifters, these features were under-resolved by the SPLASH-like release and, as a result, led to a noisier FTLEs map. Overall, agreement between the SPLASH-like and dense-grid FTLEs was still favorable in the west, where SPLASH-like fields correctly indicated, or at least hinted upon, the high-FTLE ridge entering into the domain, and to the northwest of it, where FTLEs were uniformly lower, but not so good in the east/northeast.

Finally, during the third stage of motion ($t_{end} = 4$ days), when the drifters went further offshore, SPLASH-like FTLEs showed a very clear distinction between the high values along the southeastern edge of the domain and smaller values elsewhere. There was also a small cluster of slightly elevated FTLEs in the northwest around 89.575°W , 29.05°N , as well as a few clusters of slightly negative FTLEs scattered around the domain. Comparison with the dense-grid model FTLEs revealed that the FTLEs field was dominated by 2 strongest ridges – the S-shaped ridge in the east and the very strong nearly-zonal ridge in the south. Neither of these ridges were well resolved by the SPLASH drifters, but the red cluster in the 5th row of Fig. S3 coincided roughly with the location of the S-shaped ridge. Note also that several small regions of slightly negative values present in the

SPLASH-like FTLEs maps mostly agree well with the dense-grid model fields. Overall, SPLASH-like fields at the 3rd stage correctly indicated the presence of a manifold (region of largest FTLEs) near the northern half of the southeastern edge of the release domain. However, all other, narrower FTLEs ridges visible in the dense-grid FTLEs were not resolved by the SPLASH-like release.

L and CD (Figs. S4-S5). Being measures of complexity of individual trajectories, rather than measures involving groups of trajectories, both L and CD do not depend on the release grid. (Note that the more blue-ish appearance of the southernmost filament in the dense-grid simulations (bottom panels of Figs. S4-S5) compared to the SPLASH-like simulations (2nd from bottom panels) is the plotting artefact, as some of the yellow and orange dots in that filament are hidden behind the blue dots.) Despite this advantage, SPLASH-like L - and CD -maps were still only marginally useful in identifying the dominant LCSs. Similar to the real-drifters, SPLASH-like L and CD fields at all times were dominated by a large-scale gradient, with smaller values in the north (or northeast during the initial stage of motion) and larger values in the south (or southwest at for the initial stage). All other features, which in the dense-grid model maps showed up as the sharp smaller-scale gradients embedded into the above-mentioned large-scale gradient, were not resolved by the SPASH-like simulated drifters.

V_{en} (Fig. S6). At early times, SPLASH-like encounter volume fields showed patches that did not have any counterpart in the dense-grid fields, which were flat over most of the domain. This suggests that encounter volume might not be a good option for identifying coherent structures over short time intervals when drifters did not yet have enough time to encounter many neighbors, and that SPLASH-

based encounter volume fields were severely affected by the limited number of drifters. At intermediate stage of motion ($t_{end} = 2$ days), the V_{en} fields developed significantly more in both SPLASH-like and dense-grid simulations. Specifically, going from south to north, SPLASH-like map showed very small values in the south, a region containing higher values (or perhaps 2 separate maximizing ridges) further north of it, with the values diminishing again to the north. All of these features agreed well with the dense-grid model fields, which indeed showed smallest encounter volume in the south, then 2 separate maximizing ridges in the middle part of the domain, with blue values further north. At the third stage of motion ($t_{end} = 4$ days), the dominant features were similar to those at the second stage, with additional several maximizing ridges complicating the picture. Agreement between the SPLASH-like and the dense-grid model maps was reasonably good, but distinguishing all the various individual ridges within the SPLASH-like maps became increasingly challenging with time. It is interesting to note that at 4 days the dense-grid model field showed quite a bit of yellow in the bottom left panel but seemed mostly blue in the bottom middle and right panels. This is because trajectories released in the southern (blue V_{en}) part of the release domain experienced fast separations and formed a long blue tail that visually dominated the distribution, with most non-blue values confined to the smaller area near 90°W and 28.82°N (there are a few cyan dots hidden behind dark blue in the southernmost filament but nearly all yellow values are confined to the small area). Overall, encounter volume worked best at intermediate times when the drifters had enough time to encounter their neighbors but when the dominant LCSs were not overly complex to be resolved by the SPLASH-like drifters.

D (Fig. S7). Dilation at the initial stage of motion ($t_{end} = 0.5$ days), showed a zonal stripe of larger positive values extending into the domain from the west, with smaller values to the north and south. In the very south of the domain, the values increased again. In the north, dilation decreased and became negative in the northern corner. Both the zonal stripe and the convergence region in the north agreed with their counterparts identified using FTLEs maps. Dense-grid model dilation, computed by integrating the Eulerian model divergence along trajectories released on a dense grid, was in excellent agreement with the SPLASH-like D maps. At longer times, the agreement between SPLASH-like and dense-grid model maps was still reasonably good when and where dilation could be reliably computed, but because many drifters separated from their neighbors too far and/or aligned into polygons that were overly elongated, SPLASH-like dilation fields became gappy. Overall, dilation seemed a useful diagnostic when and where it can be reliably computed, but its estimation from limited drifter data became increasingly challenging with time due to the separation and alignment of the drifters.

$LAVD$ (Fig. S8). At early times, $LAVD$ field was dominated by the large values in the south, which were clearly visible in both SPLASH-like and dense-grid model maps. There was also a stripe of slightly elevated values entering from the western corner of the domain, which was reminiscent of the features observed in the FTLEs maps. At longer times, SPLASH-like $LAVD$ field became increasingly gappy and noisy. The main features of the dense-grid $LAVD$ field at the intermediate and later stages were the blue cluster near the middle of the domain at 89.53°W , 29.3°N , the yellow filament entering the domain from the western corner, a small yellow cluster in the very south, and another yellow cluster near the southeastern

edge of the domain (which coincided with the area to the east of the letter-S-shaped filament identified in the FTLE maps). None of the yellow clusters were resolved in SPLASH-like maps, and only a hint of the low-*LAVD* region in the middle of the domain was suggested by the SPLASH-like fields. Overall, SPLASH-like *LAVD* maps were reliable at early times, as suggested by the good agreement with their dense-grid counterparts, but deteriorated significantly at later times, to the point of missing all features except a low-*LAVD* region in the middle of the domain.

SC (Fig. S9-S10). For the simulated SPLASH-like drifters (Fig. S9), the optimized-parameter spectral clustering method identified 2 cluster configurations for each time. (We remind the reader that the optimized-parameter spectral clustering algorithm sweeps through a range of values for the sparsification radius – the parameter defining the size of the resulting spectral clusters – to find optimal values that correspond to the local maxima in normalized eigengap.) At the initial stage of motion, both optimal cluster configurations consisted of 14 clusters, which is similar to the number of spectral clusters for the real drifters at early times. Also, just like in the case with real drifters, the number of clusters for simulated SPLASH-like drifters decreased with time. At the intermediate stage of motion, again 2 optimal cluster configurations were identified – one with 9 and another with 4 clusters. In both cases, the release domain was split zonally at about 29°N into a larger northern and a smaller southern cluster, with a few trajectories in the very south of the release domain assigned to their own separate clusters. When mapped to the current position of the drifters, those southern trajectories lined up along the tail part of the distribution extending to the west. In the case with 9 clusters, the large northern cluster was additionally split into two. At the third stage of motion, there were again 2 optimal cluster

configurations – with 6 and 4 clusters. For the former, most of the domain was assigned to one cluster, with the second smaller cluster containing trajectories in the east, and three very small clusters in the very south of the release domain. When mapped to the current drifter positions, the splitting pattern became more obvious, with the body of the distribution assigned to one main cluster, and with another cluster containing southern trajectories; 2 trajectories in the very north were assigned to their own clusters. For the configuration with 4 clusters, the release domain was split into 2 large clusters, with 2 trajectories in the south assigned to their own separate clusters.

The domain used in the dense-grid *SC* simulations had same minimum and maximum values for latitude and longitude as SPLASH domain, but was rectangular rather than rhomboid. As some of the LCS, such as the S-shaped manifold in the east and longitudinal manifold in the south, were confined to near the edges of the release domain, we decided to include these regions in the dense-grid simulations. For the dense-grid model spectral clusters (Fig. S10), the method also identified several optimal delineations of the domain into clusters at each time. For the early stage, all configurations had a large number of clusters (between 8 and 19), similar to the SPLASH-like spectral clustering results. In Fig. S10 we show an optimal division of the domain with the minimum (8) and maximum (19) number of clusters. At the intermediate stage of motion, there were two optimal configurations, one with 18 and another with 16 clusters. However, unlike at earlier times, many clusters were small and located on the periphery of the domain, outside of the SPLASH-like release domain in Fig. S9. Thus, despite the overall large number of clusters identified at the intermediate stage of motion, the number of clusters within the SPLASH domain was significantly smaller than at the early stage, which agrees well with the

SPLASH-like results. In particular, the configuration with 16 clusters assigned the entire SPLASH domain to one cluster, whereas the configuration with 18 clusters divided the SPLASH domain into two clusters, with the division curve at near 29°N , similar to the results for the SPLASH-like simulated drifters in Fig. S9. The situation at 4 days is in many aspects similar to that at 2 days. Specifically, the optimized-parameter spectral clustering identified several optimal configurations with a large number of clusters, from 7 to 17. However, in all of these configurations, a large number of small clusters were located near the southern edge of the domain, outside of the SPLASH domain in Fig. S9, with the bulk of the SPLASH domain assigned to just one cluster (a representative spectral cluster configuration at 4 days is shown in the bottom row of Fig. S10). To summarize, at early times, both SPLASH-like and dense-grid simulations resulted in splitting the SPLASH release domain into a large number of clusters, although the exact splitting was different between the two simulations. At later times (both at intermediate and late stages), the number of clusters present within the SPLASH domain dropped significantly. Compared to the SPLASH-like simulations, dense-grid simulations identified several additional clusters in the south and in the northwestern corner, all laying outside of the SPLASH domain. At the intermediate stage, both SPLASH-like and dense-grid simulations produced a configuration with the split along 29°N . At later stage, both SPLASH-like and dense-grid simulations produced a configuration, where most of the SPLASH domain was assigned to just one cluster (blue).

In additional simulations (not shown), we have also investigated the robustness of all dynamical systems quantities to the GPS positioning noise in the drifter data by adding a random displacement (taken from a normal distribution with standard deviation of 5 m) to

the simulated drifter trajectories in the NCOM model. Not surprisingly, such noise had a negligible effect on FTLEs, V , and spectral clusters (because 5 m is negligible compared to the distances between the drifters), had a weak effect on L and CD (because these are integral quantities of the differences in sequential drifter positions), and a stronger effect on D and $LAVD$ (both because these are integral quantities and because the position disturbance of 5 m may be significant for the estimation of the local derivatives of velocity). When working with noisy data, applying a smoothing filter to the drifter trajectories, for example, a running average, as was done in Rypina et al. (2021) or the trajectory filtering method developed by Yaremchuk & Coelho (2014), may suppress noise, reduce errors in divergence and vorticity, and improve D and $LAVD$ estimates.

References

- Beron-Vera, F. J. and LaCasce, J. H.: Statistics of simulated and observed pair separations in the Gulf of Mexico, *J. Phys. Oceanogr.*, 46, 2183–2199, 2016.
- Jacobs, G. A., Bartels, B. P., Bogucki, D. J., Beron-Vera, F. J., Chen, S. S., Coelho, E. F., Curcic, M., Griffa, A., Gough, M., Haus, B. K., and Haza, A. C.: Data assimilation considerations for improved ocean predictability during the Gulf of Mexico Grand Lagrangian Deployment (GLAD), *Ocean Model.*, 83, 98–117, 2014.
- Martin, P. J. Description of the navy coastal ocean model version 1.0, Naval Research Lab Stennis Space Center, MS, 2000.
- Özgökmen, T. M., Bracco, A., Chassignet, E. P., Chang, H., Chen, S. C., D’Asaro, E., Fox-Kemper, B., Haza, A. C., Jacobs, G., Novelli, G., and Poje, A.: Basin-Scale and Near-Surface Circulation in the Gulf of Mexico, in: International Oil Spill Conference, vol. 1, 686903, <https://doi.org/10.7901/2169-3358-2021.1.686903>, 2021.
- Poje, A. C., Özgökmen, T. M., Lipphardt, B. L., Haus, B. K., Ryan, E. H., Haza, A. C., Jacobs, G. A., Reniers, A. J. H. M., Olascoaga, M. J., Novelli, G., and Griffa, A.: Submesoscale dispersion in the vicinity of the Deepwater Horizon spill, *P. Natl. Acad. Sci. USA*, 111, 12693–12698, 2014.
- Rypina, I. I., Getscher, T. R., Pratt, L. J., and Mourre, B.: Observing and quantifying ocean flow properties using drifters with drogues at different depths, *J.*

Phys. Oceanogr., 51, 2463–2482, 2021.
Yaremchuk, M. and Coelho, E. F.: Filtering drifter
trajectories sampled at submesoscale resolution, IEEE

J. Oceanic Eng., 40, 497–505, DOI:
10.1109/JOE.2014.2353472, 2014.

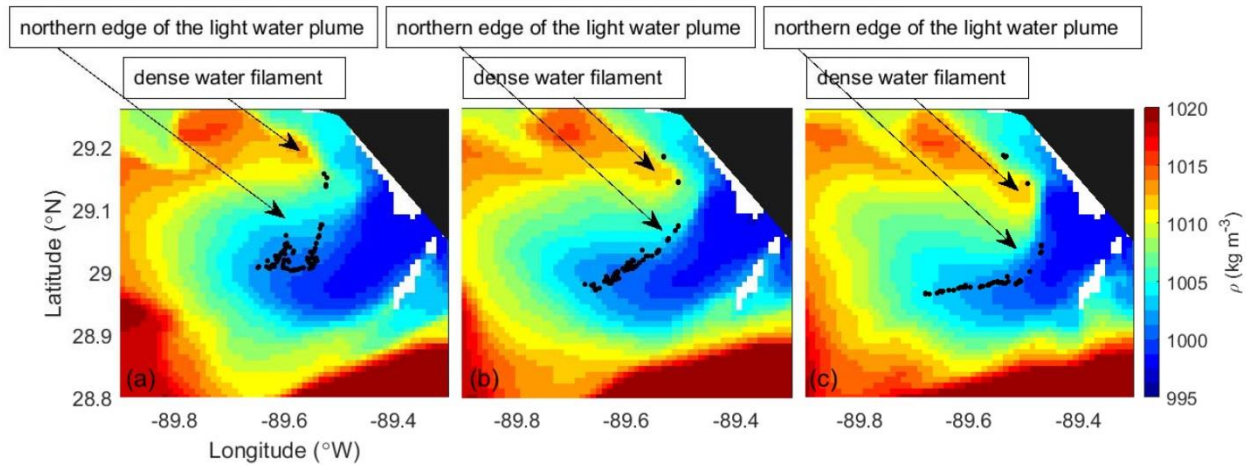


Figure S1. SPLASH drifter positions superimposed on the model surface density fields on days (a) 1; (b) 1.25; and (c) 1.5 after the release.

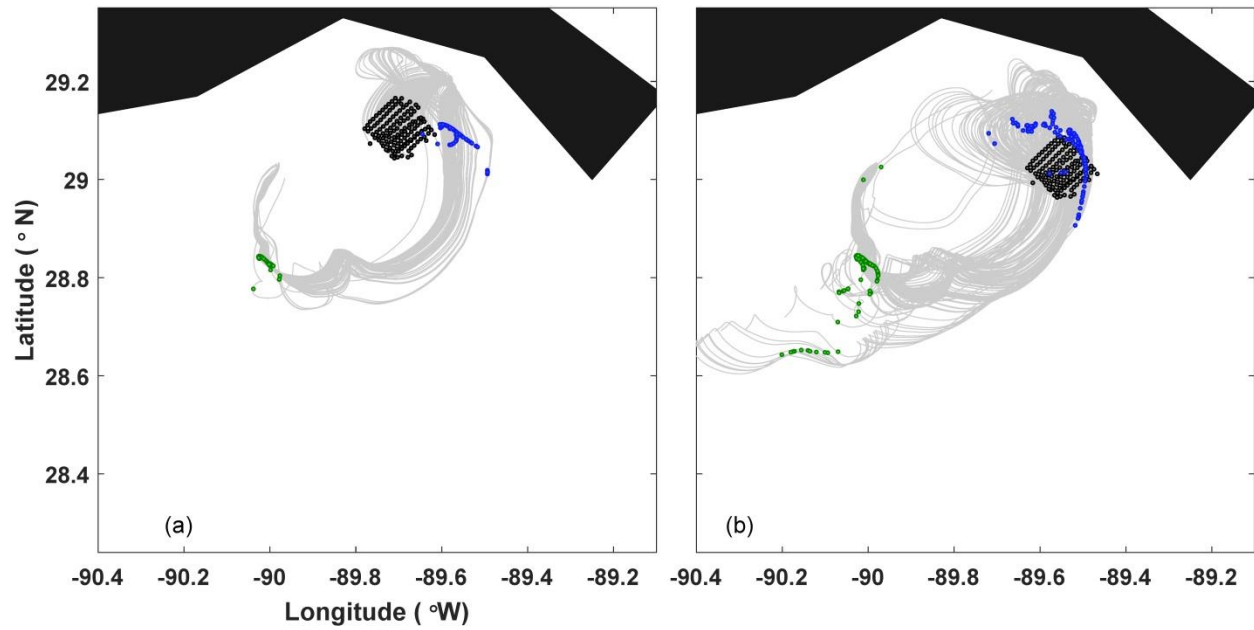


Figure S2. (a) Trajectories of the NCOM-simulated drifters released at the times and locations of the real SPLASH drifters, with the positions at the release time, 2 days, and 4 days shown by black, blue and green dots, respectively. Trajectories of the NCOM-simulated drifters released at the slightly shifted locations, with the positions at the release time, 2 days, and 4 days shown by black, green and blue dots.

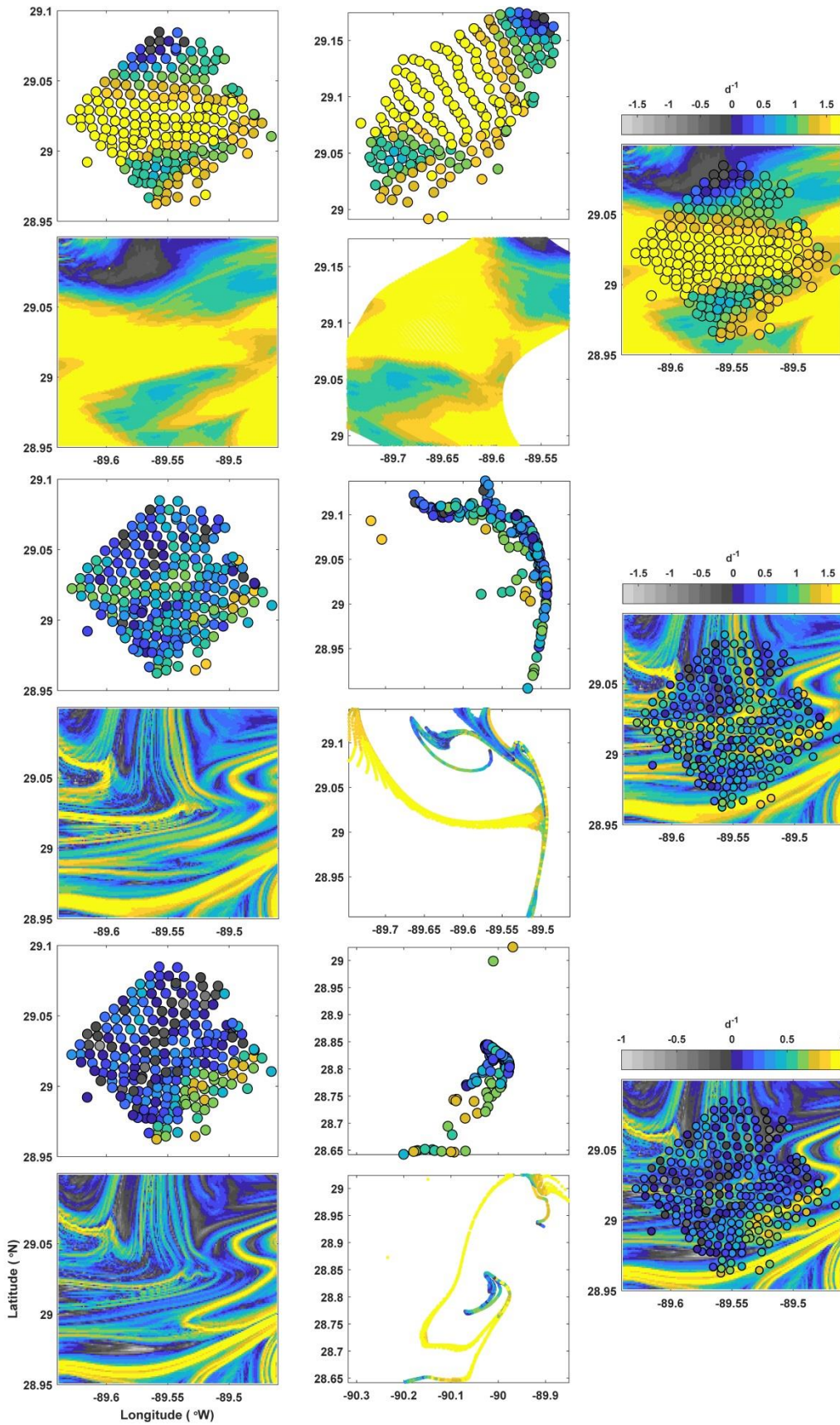


Figure S3. Model-based FTLEs at 0.5 (rows 1-2), 2 (rows 3-4) and 4 (rows 5-6) days for simulated SPLASH drifters (rows 1,3,5) and for drifters released on a dense regular orthogonal grid (rows 2,4,6). Fields are mapped to the initial (left and right) and current (middle) positions of the simulated drifters. SPLASH-like and dense-grid simulations are superimposed in the right panel to simplify comparison.

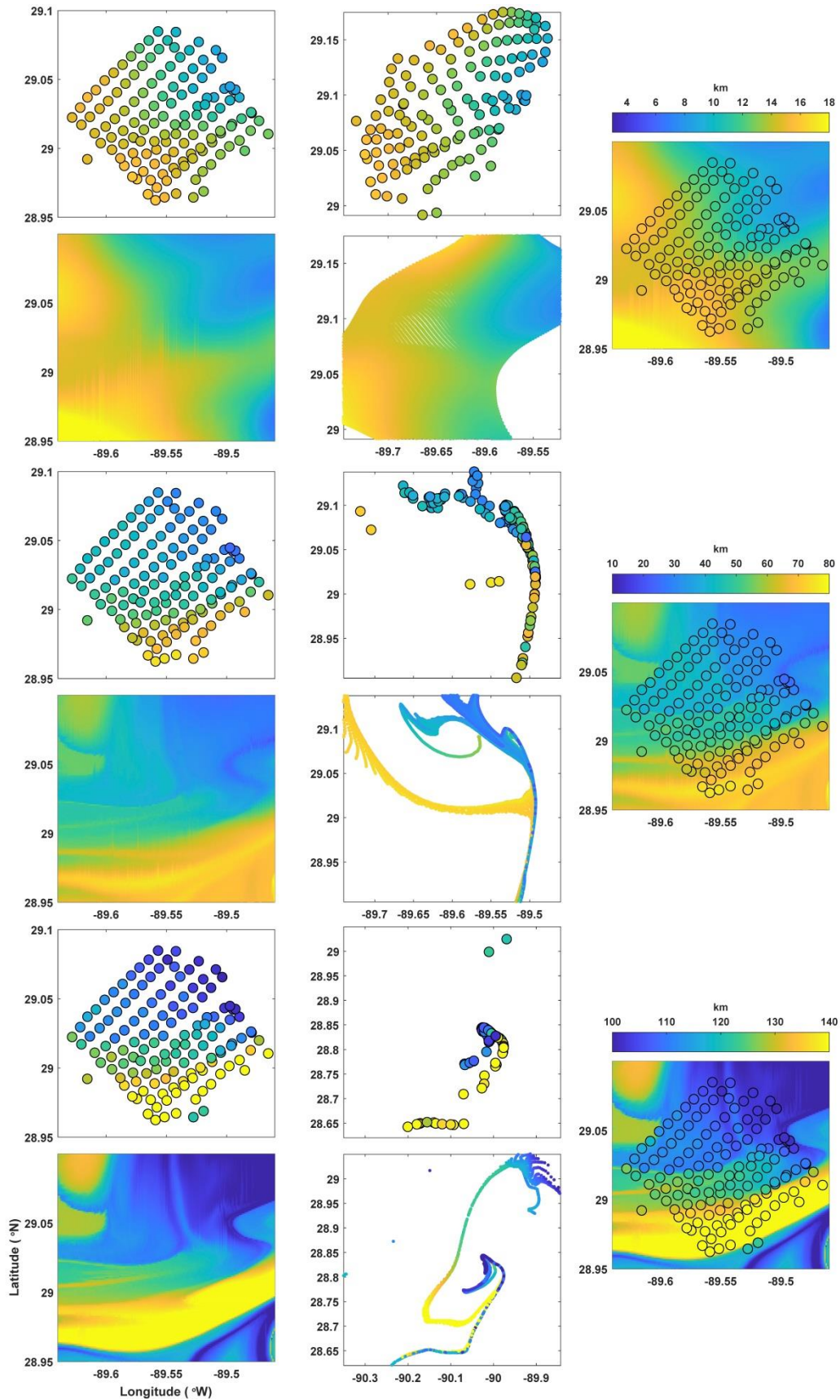


Figure S4. Model-based path length at 0.5 (rows 1-2), 2 (rows 3-4) and 4 (rows 5-6) days for simulated SPLASH drifters (rows 1,3,5) and for drifters released on a dense regular orthogonal grid (rows 2,4,6). Fields are mapped to the initial (left and right) and current (middle and right) positions of the simulated drifters. SPLASH-like and dense-grid simulations are superimposed in the right panel to simplify comparison.

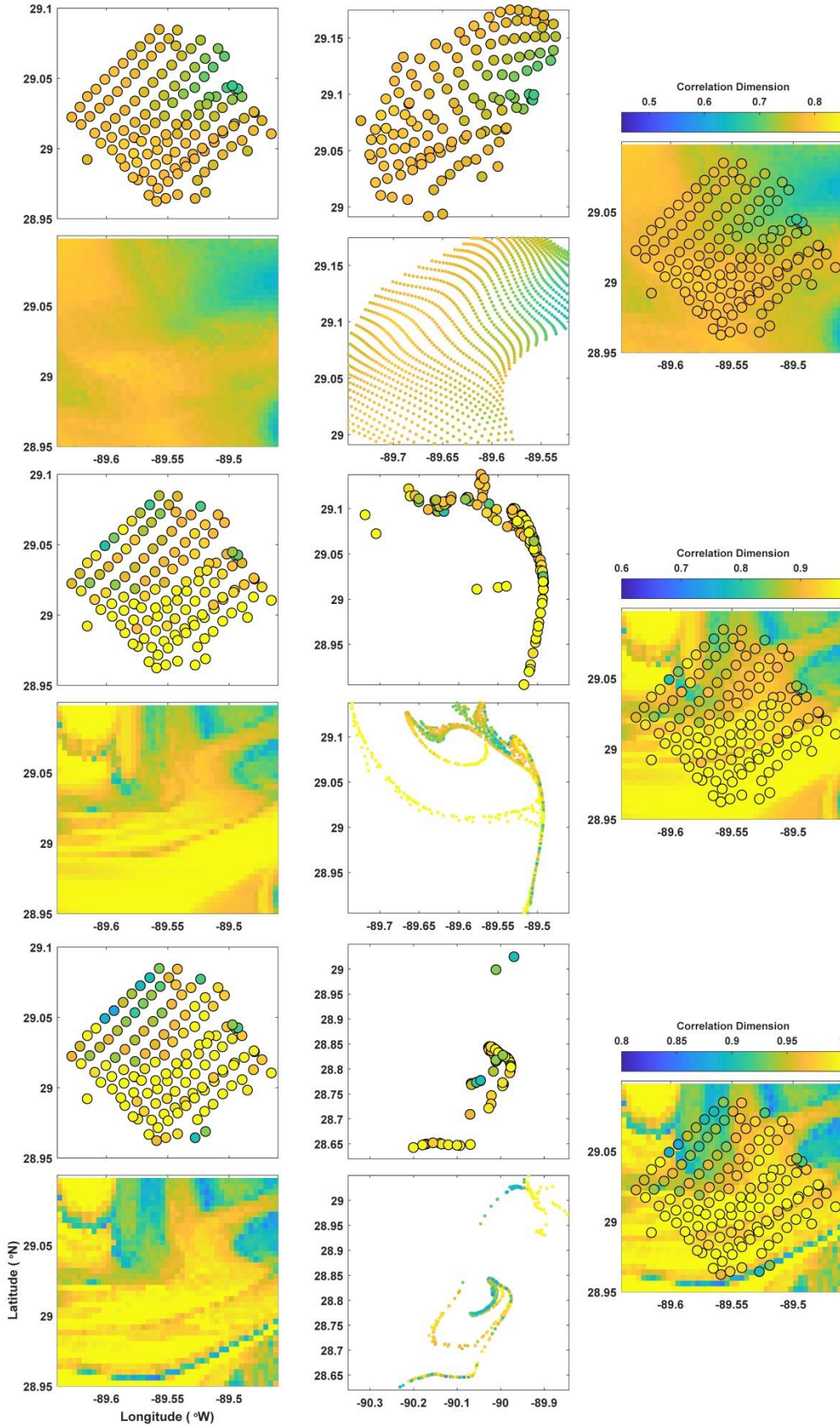


Figure S5. Model-based correlation dimension at 0.5 (rows 1-2), 2 (rows 3-4) and 4 (rows 5-6) days for simulated SPLASH drifters (rows 1,3,5) and for drifters released on a dense regular orthogonal grid (rows 2,4,6). Fields are mapped to the initial (left and right) and current (middle and right) positions of the simulated drifters. SPLASH-like and dense-grid simulations are superimposed in the right panel to simplify comparison.

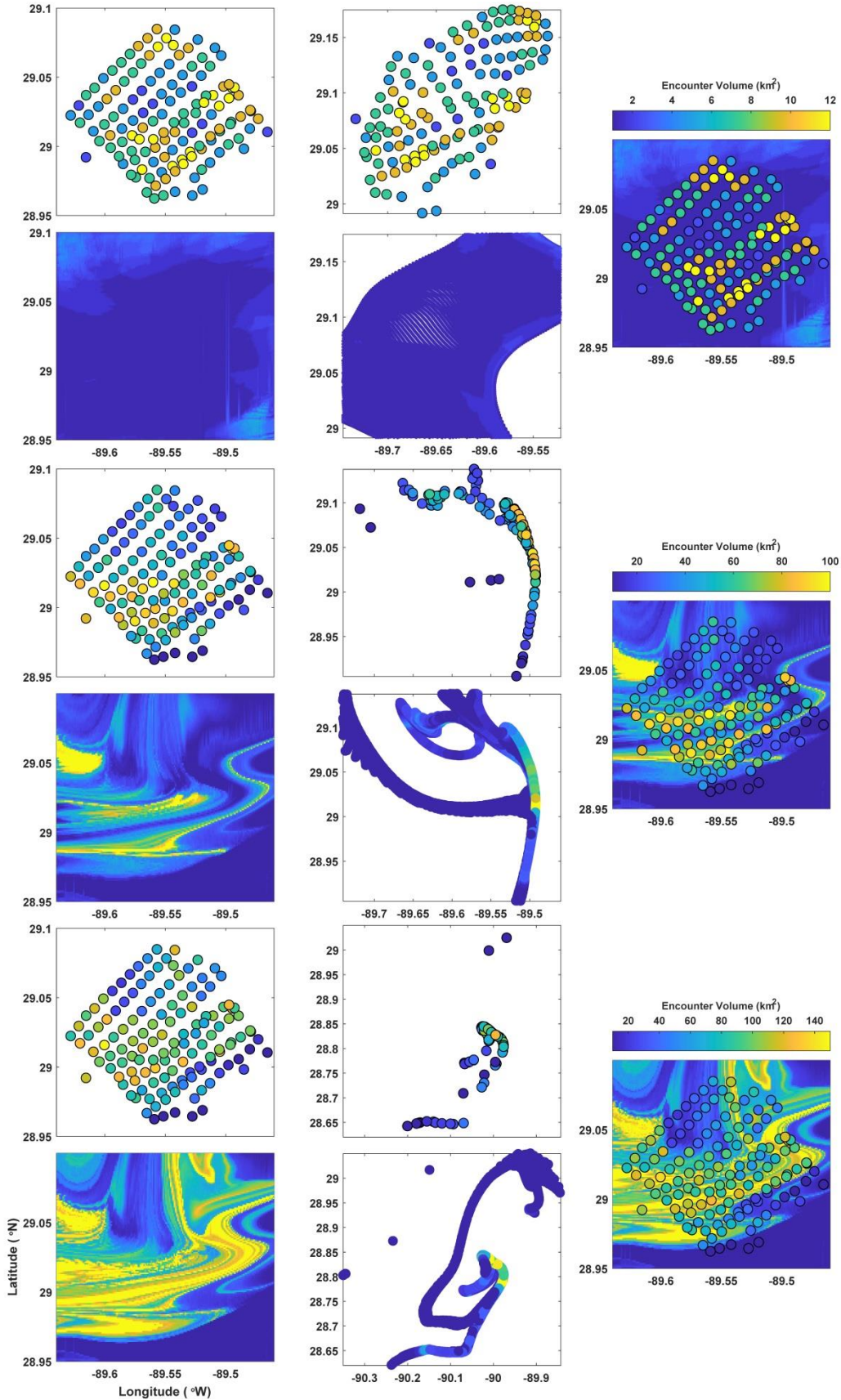


Figure S6. Model-based encounter volume at 0.5 (rows 1-2), 2 (rows 3-4) and 4 (rows 5-6) days for simulated SPLASH drifters (rows 1,3,5) and for drifters released on a dense regular orthogonal grid (rows 2,4,6). Fields are mapped to the initial (left and right) and current (middle and right) positions of the simulated drifters. SPLASH-like and dense-grid simulations are superimposed in the right panel to simplify comparison.

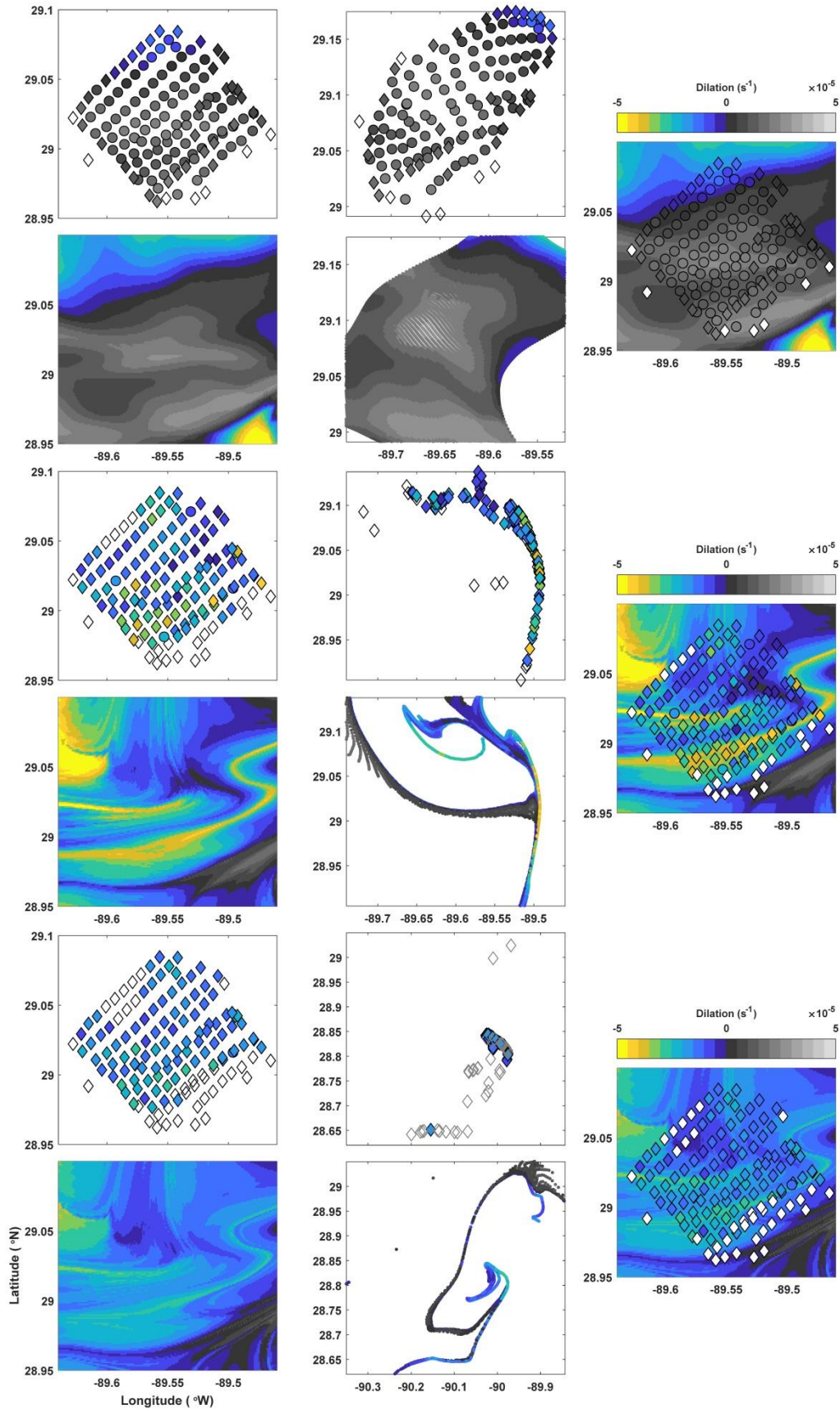


Figure S7. Model-based dilation at 0.5 (rows 1-2), 2 (rows 3-4) and 4 (rows 5-6) days for simulated SPLASH drifters (rows 1,3,5) and for drifters released on a dense regular orthogonal grid (rows 2,4,6). Fields are mapped to the initial (left and right) and current (middle and right) positions of the simulated drifters. SPLASH-like and dense-grid simulations are superimposed in the right panel to simplify comparison. Colormap as in Fig. 7.

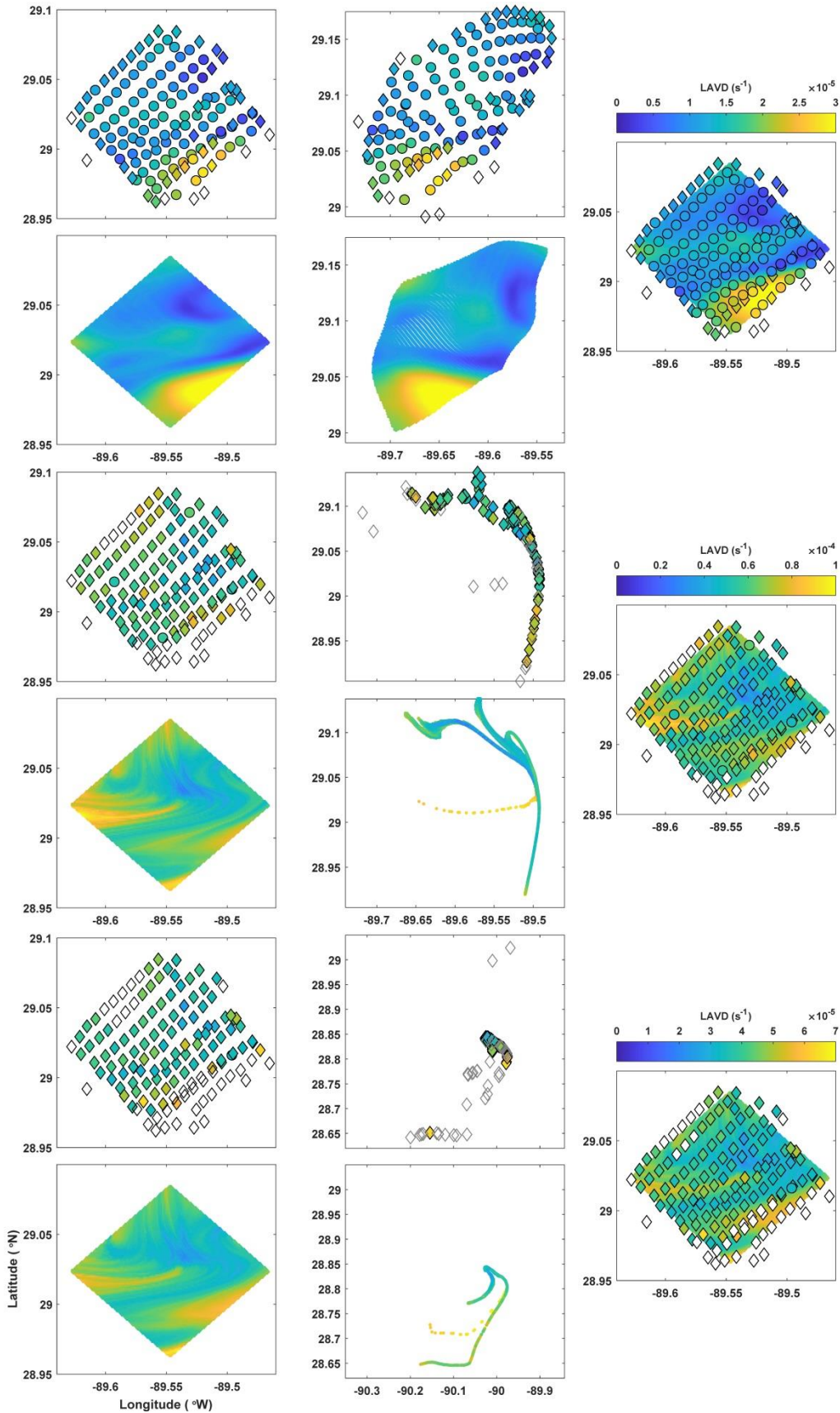


Figure S8. Model-based LAVD at 0.5 (rows 1-2), 2 (rows 3-4) and 4 (rows 5-6) days for simulated SPLASH drifters (rows 1,3,5) and for drifters released on a dense regular orthogonal grid (rows 2,4,6). Fields are mapped to the initial (left and right) and current (middle and right) positions of the simulated drifters. SPLASH-like and dense-grid simulations are superimposed in the right panel to simplify comparison.

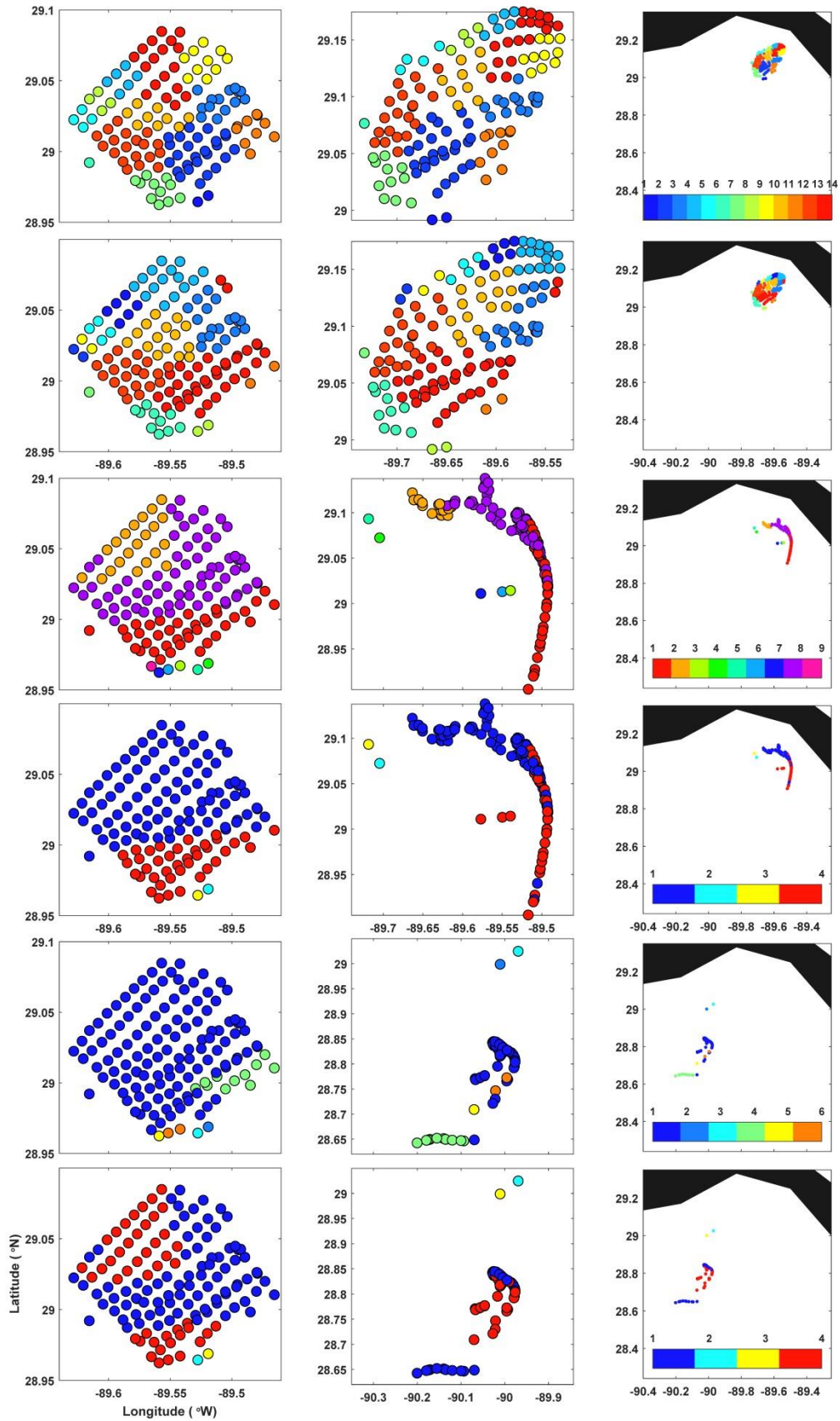


Figure S9. Spectral clusters for simulated SPLASH drifters at $T=0.5$ days (rows 1-2); $T=2$ days (rows 3-4); and $T=4$ days (rows 5-6). Fields are mapped to the initial (left) and current (middle and right) positions of the simulated drifters.

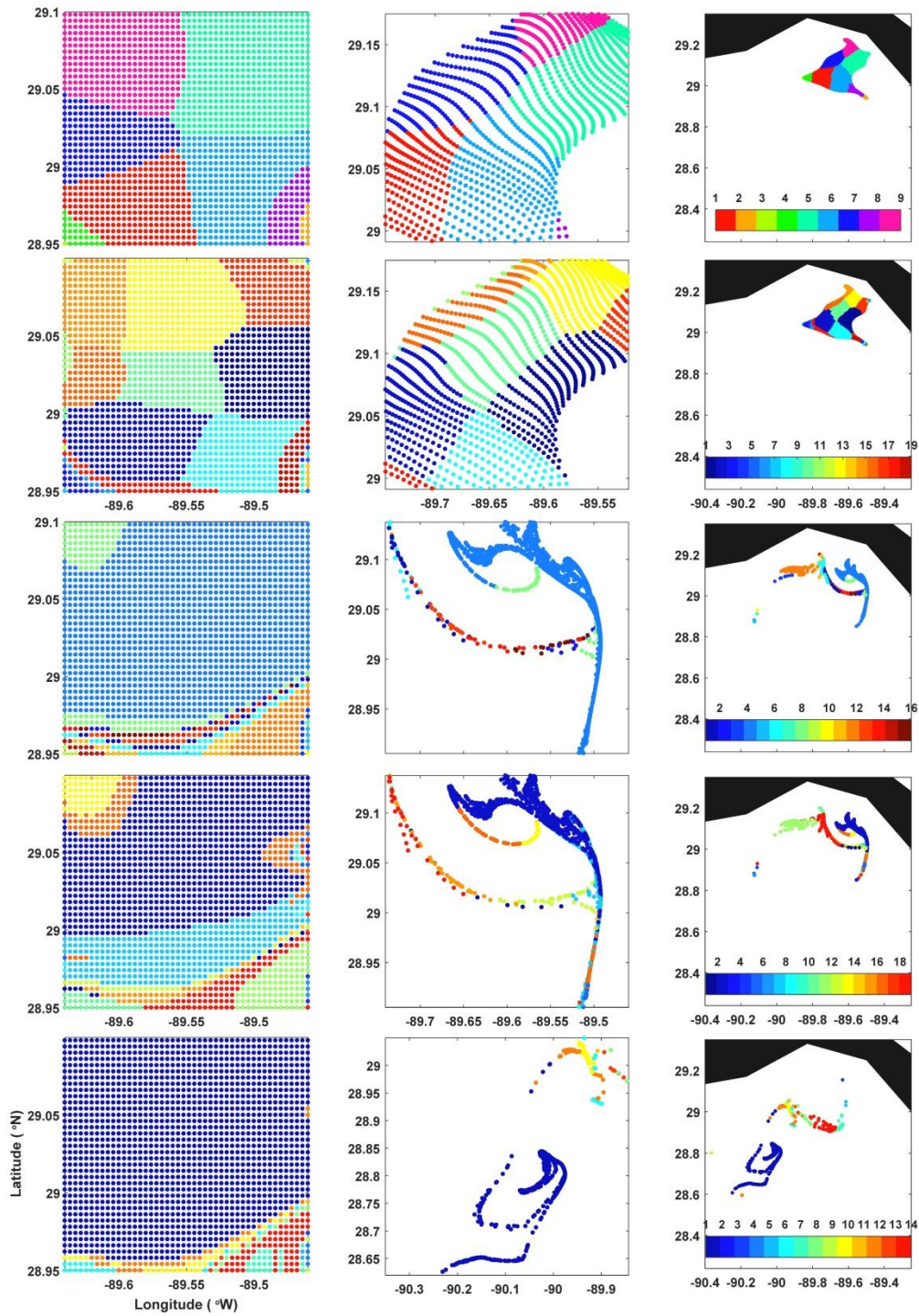


Figure S10. Dense-grid model spectral clusters computed using simulated trajectories released on a dense regular grid at $T=0.5$ (rows 1-2); 2 days (rows 3-4); and 4 days (row 5). Fields are mapped to the initial (left) and current (middle and right) positions of the simulated drifters.